

Cite this: DOI: 00.0000/xxxxxxxxxx

Integrating anaerobic digestion and slow pyrolysis improves the product portfolio of a cocoa waste biorefinery†

Stef Ghysels,^{ab‡} Nayaret Acosta,^{ab‡} Adriana Estrada,^a Mehmet Pala,^a Jo De Vrieze,^a Frederik Ronsse,^b and Korneel Rabaey^a

Received Date

Accepted Date

DOI: 00.0000/xxxxxxxxxx

The integration of conversion processes with anaerobic digestion is key to increase value from agricultural waste, like cocoa pod husks, generated in -developing- countries. The production of one metric ton of cocoa beans generates some 15 metric tonnes of organic waste that is today underutilized. This waste can be converted into added value products by anaerobic digestion, converting part of the cocoa pods to biogas while releasing nutrients, and pyrolysis. Here, we compared different scenarios for anaerobic digestion/slow pyrolysis integration in terms of product portfolio (*i.e.*, biogas, pyrolysis liquids, biochar and pyrolysis gases), energy balance and potential for chemicals production. Slow pyrolysis was performed at 350 °C and 500 °C on raw cocoa pod husks, as well as on digestates obtained from mono-digestion of cocoa pod husks and co-digestion with cow manure. Anaerobic digestion resulted in 20 to 25 wt.% of biogas for mono and co-digestion, respectively. Direct pyrolysis of cocoa pod husks mainly resulted in biochar with a maximum yield of 48 wt.%. Anaerobic digestion induced compositional changes in the resulting biochar, pyrolysis liquids and evolved gases after pyrolysis. Pyrolysis of mono-digestate *e.g.*, resulted in a more energy-dense organic phase, rich in valuable phenolics while poorer in light oxygenates that hold a modest value. Our comparison shows that co-digestion/slow pyrolysis at 500 °C and mono-digestion/slow pyrolysis at 350 °C both present high-potential biorefinery schemes. They can be self-sustaining in terms of energy, while resulting in high quality biochar for nutrient recycling and/or energy recovery, and/or phenolics-rich pyrolysis liquids for further upgrading into biorefinery intermediates.

1 Introduction

Agricultural residues hold potential as resources for the recovery of energy, chemicals and materials in a biorefinery concept, without competing for land-use for primary food production^{1–3}. Anaerobic digestion is a rather simple platform, typically employed to convert *e.g.*, manure or dedicated energy crops into biogas for energy, whereby the initial mass of the bio-waste is effectively reduced⁴. Single conversion processes (*i.e.*, electrochemical, biological, physical and thermochemical) for bio-waste are typically separately studied. However, the integration of these processes with anaerobic digestion in particular is of increasing interest to enhance the profitability of anaerobic digestion⁵.

Clark⁶, Wang *et al.*⁷, Choudhary *et al.*⁸ indeed highlighted that such investigations are crucial to fully explore bio-waste's potential as biorefinery feedstock.

Moreover, biorefining of agricultural residues can generate additional value for (developing) countries, where these agricultural residues are generated. In that context, pyrolysis is another rather simple process that can convert anaerobic digestion residues (*i.e.*, digestate) into value-added products at an elevated temperature in an oxygen-free atmosphere. Similar studies on pyrolysis of lignocellulosic fermentation residues learn that carbohydrates are rather selectively converted in the biological process, leaving a lignin-enriched residue which is converted to typical lignin-derived pyrolysis products, being biochar and phenolics-rich liquids^{9–12}. While similar product distributions can be expected for anaerobic digestion/pyrolysis of agricultural residues, most studies focus on maximal energy recovery by combusting biogas and pyrolysis products^{13,14}. The characterisation of end-products from anaerobic digestion/pyrolysis and the evaluation of their potential application besides combustion are often overlooked. In an agricultural context, biochar can be reallocated to the field to recycle nutrients and to sequester carbon¹⁵. On the other

^a Centre for Microbial Ecology and Technology (CMET), Ghent University, Coupure Links 653, B-9000 Ghent, Belgium; Tel: +32 9264 5976;

E-mail: Korneel.Rabaey@UGent.be

^b Thermochemical Conversion of Biomass Research Group, Department of Green Chemistry and Technology, Ghent University, Coupure Links 653, 9000 Ghent, Belgium; E-mail: Stef.Ghysels@UGent.be

† Electronic Supplementary Information (ESI) available: [details of any supplementary information available should be included here]. See DOI: 00.0000/00000000.

‡ These authors contributed equally to this work

hand, phenolics in the phenolics-rich liquids can be upgraded to various platform chemicals¹⁶.

This study therefore investigates an integrated anaerobic digestion/slow pyrolysis scheme for the valorisation of agricultural residues, using cocoa pod husks as an example case. It was hypothesised that anaerobic digestion first converts carbohydrates into useful biogas¹⁷, which decreases the conversion of these carbohydrates into less-valuable oxygenated compounds after pyrolysis. Similarly, the largely unconverted lignin-enriched digestate after anaerobic digestion was hypothesised to result in biochar and phenolics-rich pyrolysis liquids. Cocoa pod husks were used in this study, as this agricultural residue is produced at high quantities and is currently underexplored as feedstock for valorisation (as elaborated below). Slow pyrolysis conditions were applied in this work to maximize biochar yield¹², hence, the potential for carbon sequestration and nutrient recycling.

The annual worldwide production of cocoa beans amounts to 4 million metric tonnes, of which Ecuador, the origin of the herein used cocoa pod husks produced 232 000 metric tonnes¹⁸. Cocoa pod husks encompass the largest residue for which currently only limited valorisation schemes have been explored. Cocoa pod husks represent between 70% to 80% in dry weight of the fruit¹⁹. If left unattended on the field for nutrient recycling, pathogens, such as e.g., *Marasmius pernicius*, can cause pod rot, which in turn can damage the plantation, cause odour-related problems and uncontrolled emissions of methane into the atmosphere^{20,21}.

Alternatively, incineration of cocoa pod husks can be considered²², but if improperly managed, this results in considerable air pollution through the emission of fine particulate dust, NO_x and noxious compounds, like furans. Even with air pollution control and energy recovery, effective incineration is still hampered by the inherent high-ash content of the cocoa pod husks²³. The ash can cause slagging upon incineration, while the retained bottom ashes typically end up in landfills, although applications for valorisation of these bottom ashes are being investigated²³.

Significant value creation was therefore pursued through direct anaerobic digestion, slow pyrolysis and their integration. Only a handful of studies exist, where cocoa pod husks were subjected to either anaerobic digestion, either pyrolysis, while no studies exist on their integration.

Cocoa pod husks, like other lignocellulosic biomasses, are converted to biogas upon digestion to only a modest extent²⁴. In many cases, the methane yield after anaerobic digestion of lignocellulosic biomass only amounted to 60% of what theoretically can be expected. Co-digestion with manure, like in Dahunsi *et al.*²⁵, Acosta *et al.*²⁶, proved effective to obtain elevated biogas yields without any pretreatment¹⁷. Therefore, mono-digestion (i.e., using only cocoa pod husks) and co-digestion with cow manure were investigated in this work.

Regarding pyrolysis of cocoa residues, both fast pyrolysis and slow pyrolysis studies have been reported^{27–29}. Comprehensive comparison of these different studies is however hampered by inconsistencies in reporting product yields and/or analysis techniques. For instance, Adjin-Tetteh *et al.*²⁸ only analysed the composition of a silylated single-phase pyrolysis liquid, reporting only long-chain fatty acids and their derivatives (e.g., octanoic acid and

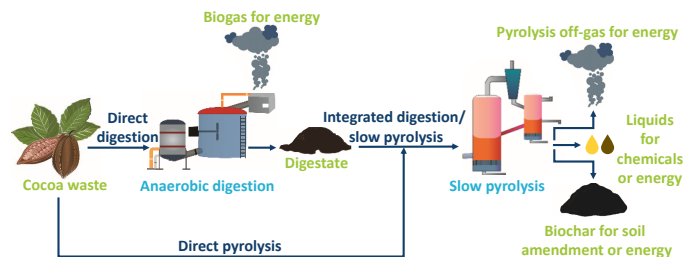


Fig. 1 Overview of the herein studied processes and/or combinations thereof: anaerobic digestion, slow pyrolysis and the anaerobic digestion/slow pyrolysis integrated process.

9,12-octadecadienoic acid).

Overall, while integrated anaerobic digestion/slow pyrolysis can generally increase the overall profitability, no specific studies exist on the integration of anaerobic digestion and pyrolysis of cocoa pod husks, despite the large quantities of this waste. This work therefore illustrates integrated anaerobic digestion/slow pyrolysis for cocoa pod husks by evaluating the individual processes (“direct digestion” and “direct pyrolysis” in Fig. 1) and the integration of both (“integrated digestion/slow pyrolysis” in Fig. 1). Each valorisation scheme’s product portfolio and value is carefully evaluated in this work to aid the management of this particular voluminous waste.

2 Experimentation

2.1 Cocoa pod husks and digestates

Cocoa pods were obtained from Manabí province in Ecuador. The term mono-digestate indicates the effluent from three lab-scale mesophilic anaerobic digesters with cocoa waste as sole feedstock. Co-digestate denotes the liquid effluent from three lab-scale mesophilic anaerobic digesters, with cocoa waste and cow manure as feedstocks in a ratio of 3:1 (on the volatile solids, or VS, content). The reactors for mono and co-digestion were operated for 117 days in Schott bottles (400 mL functional volume) at mesophilic conditions (35 ± 1 °C) in biological triplicates. The organic loading rate (OLR) was increased stepwise from 1 to 4 g VSS · L⁻¹ · day⁻¹. Prior to pyrolysis, the cocoa pods and digestates were sun-dried for 24 hours on-site and additionally dried at 105 °C for 72 hours to prevent microbial activity.

2.2 Experimental setup and procedures

Slow pyrolysis experiments were conducted, applying a constant heating rate of ca., 10 °C · min⁻¹ to 350 °C or 500 °C, with a holding time of one hour upon reaching the desired temperature. The lowest pyrolysis temperature was chosen based on literature thermogravimetric data. At 350 °C, the peak temperature of maximum mass-loss (being ca., 300 °C) was exceeded, achieving a mass loss of ca., 66 wt.%^{30,31}. Therefore, 350 °C was regarded the lowest temperature at which a devolatilised (hence, charred) feedstock was expected. The pyrolysis temperature of 500 °C is a typical higher-end slow pyrolysis temperature³².

A fully controlled lab-scale setup for fast pyrolysis³³ was reconfigured to conduct slow pyrolysis (Supplementary Information).

The average of three K-type thermocouple readings from within the setup was used to indicate the temperature inside the feedstock container). A mass of 50 g cacao pod husks or digestate (particle size between 0.5 to 2 mm) were loaded to a fixed bed reactor. This fixed bed was continuously purged with nitrogen gas ($\geq 99.8\%$ purity, industrial, Air Liquide, Belgium) at a rate of $20 \text{ L}_N \cdot \text{h}^{-1}$. The entrained pyrolysis vapours were condensed in a metal-jacketed condenser and glass condenser, both cooled with water of 2°C .

Uncondensed vapours were subsequently swept along a cotton wool and activated carbon filter to trap fine dust particles and residual uncondensed aerosols to prevent damage to the dry gas meter (Itron Gallus, Germany). After registering the volumetric flow rate of evolved non-condensable gases, the stream was split. One fraction went to the vent, while the other fraction was collected into a gas collection bag (2 L) for compositional analysis. During slow pyrolysis, the quantity of evolved pyrolysis vapours changes in function of the reactor temperature (also apparent through literature thermogravimetric analysis), while the gas composition is also non-constant over the course of time (temperature). This heterogeneity was accounted for by replacing the gas bag at specific times (e.g., one bag with collected gases between ambient temperature and a pyrolysis temperature of 250°C , a second bag for gases evolving between 250°C and 300°C , and from that point forward, every 50°C).

2.3 Feedstock and product analyses

2.3.1 Proximate analysis.

Moisture content (MC), volatile matter (VM) content, ash content and fixed carbon (FC) content were determined in technical triplicates for cocoa pod husks, mono and co-digestate and their corresponding biochars, according to Enders and Lehmann³⁴. Briefly, the moisture content of the sample was determined by placing the feedstock or biochar in a drying oven at 105°C for 2 h and recording the weight difference. The VM was released by heating the covered crucibles in a muffle furnace at 950°C (9 min), after which the weight loss was recorded after the samples cooled in a desiccator. Finally, the same samples were heated to 750°C and maintained for 8 h to quantify the ash after cooling in a desiccator. The fixed carbon content (FC) was calculated by difference. The mass fractions of VM and FC were calculated on a dry (db), and on a dry-and-ash-free (daf) basis. The latter was to only consider the organic matrix within the cocoa pod husks. The ash recovery was calculated from the ash content of the feedstock and of the biochar, and the biochar yield as in Ghysels *et al.*¹¹.

2.3.2 Elemental analysis.

Elemental analysis was performed in technical duplicates, using a Flash 2000 Elemental Analyzer (Thermo Fisher Scientific, Waltham, MA, USA). Samples were ground and *ca.*, 1.5 mg was used for each analysis. Elements C, H, N and S were measured, while the oxygen content was obtained by difference. 5-Bis(5-tert-butyl-benzoxazol-2-yl)thiophene (BBOT) was used as standard reference.

2.3.3 Higher heating value (HHV).

The HHV of the cocoa waste, mono-digestate and all biochars were determined in duplicate with an E2k Combustion Calorimeter (Digital Data Systems, PTY, Ltd.), using benzoic acid as standard reference. The energy content of the cocoa pod husks/cow manure mixture was based on the empirical chemical formula of that cocoa pod husks/cow manure mixture ($\text{CH}_{1.4}\text{O}_{1.4}\text{N}_{0.031}$). This was in turn derived from the elemental composition of cocoa pod husks (this work) and cow manure³⁵ individually, and the known ratio of cocoa pod husks and cow manure, being 3:1 on a VSS basis. The well-established relation reported by Channiwalla and Parikh³⁶ was used to obtain the HHV from the elemental composition.

The HHV of both the organic and aqueous phase pyrolysis liquids were calculated using the same correlation from Channiwalla and Parikh³⁶, based on elemental analysis of both pyrolysis liquid phases. The calorific value of biogas and non-condensable gases were calculated from the standard calorific values of their constituents³⁷ and their experimentally obtained quantity and composition. All the calorific values were expressed as $\text{MJ} \cdot \text{kg}^{-1}$ product or feedstock.

2.3.4 pH in suspension.

Dried samples of cocoa pod husks, digestate or biochar (5.0 g) were placed in a 100 mL glass beaker, to which 50 mL of deionized water was added. The suspension was mechanically stirred for 1 h at 20°C , after which the suspension was allowed to stabilize for 30 minutes prior to the pH measurement using a pH meter C532 (Consort, Turnhout, Belgium). The pH was measured in technical triplicates.

2.3.5 Concentration of Pb and Cd by ICP-OES.

The concentration of Pb and Cd was measured through inductively coupled plasma optical emission spectrometry (ICP-OES), using a Perkin Elmer 7000 DV. Approximately 20 mg of the cocoa pod husks, mono- and co-digestate, and their corresponding biochars were chemically digested with HNO_3 (8 mL, 65 wt%) in a microwave oven at to 200°C for 10 min, followed by an incubation at 200°C for 15 min. Subsequently, the HNO_3 solution (2 wt% in water) was added to a total volume of 50 mL, diluted ten times with deionised water and put into glass vials for ICP-OES analysis. The detection limits for Pb and Cd were $3 \mu\text{g} \cdot \text{kg}^{-1}$ and $0.7 \mu\text{g} \cdot \text{kg}^{-1}$, respectively.

2.3.6 GC-MS analysis of pyrolysis liquids.

The chemical composition of the organic phase of pyrolysis liquids were determined in a GC-MS (Thermo Fisher Scientific Trace GC Ultra and Thermo ISQ MS) as in Ghysels *et al.*³⁸. A volume of 100 μL of internal standard (fluoranthene in acetonitrile, 2.5 wt.%) and 5 g of acetonitrile were added to 0.20-0.25 g of each liquid sample. The sample was filtered with a $0.45 \mu\text{m}$ PTFE syringe filter and 1 μL was injected in the GC (injector temperature of 250°C , split ratio of 1:100) and separated on a chromatographic column (RTX-1701: Restek, L= 60 m; $d_i = 0.25 \text{ mm}$; $d_f = 0.25 \mu\text{m}$). Determination of the pyrolysis liquid composition was done in technical duplicates. Helium was applied as a carrier gas with

a constant column flow rate of $1 \text{ mL} \cdot \text{min}^{-1}$. The temperature program of the GC oven was as follows: (i) three minutes at constant temperature of 40°C , (ii) heating to 280°C at $5^\circ\text{C} \cdot \text{min}^{-1}$ and (iii) one minute at constant temperature of 280°C . All organic phase samples were analysed through GC-MS, while only one aqueous phase sample was analysed (from pyrolysis of cocoa pods at 350°C). The high-water content of these aqueous phase samples (*vide infra*) could negatively impact the performance of the GC-MS.

The GC-MS was calibrated with a set of reference compounds typically found in pyrolysis liquids, which were quantified directly. Chemical compounds for which the GC-MS was not directly calibrated were quantified by using representative response factors from calibrated compounds having structural similarity or which belong to the same chemical group³⁹. Considered chemical groups, containing compounds with structural similarity, were e.g.,: (i) light oxygenates (e.g., acetic acid, 1-hydroxy-2-propanone, 4-hydroxybutanoic acid, propanoic acid, 2-furanmethanol and butanoic acid) and (ii) methoxyphenols (e.g., 2-methoxyphenol, 2,6-dimethoxy phenol). A complete list is included in Supplementary Information, Table A1.

2.3.7 Water content of aqueous pyrolysis liquids.

The water content of the aqueous phases was analysed by Karl Fischer titration (Mettler Toledo V20, 5 ml burette, electrode: DM 143-SC, reagent: Merck Combi Titrant 5 Keto and solvent: Merck Combi Solvent 5 Keto). The water content of the sample (0.01 - 0.03 g) was calculated by the titrator. The analysis of the samples was performed in technical duplicates.

2.3.8 Non-condensable gases composition.

Non-condensable gases were separated on a micro GC (Varian Micro-GC 490-GC) with two analytical columns: a 10 m Mole-sieve 5A (with backflush) and a 10 m PPU with thermal conductivity detectors, using helium as carrier gas ($\geq 99.999\%$ purity, Air Products, Belgium). Eight different gases were separated: H_2 , O_2 , N_2 , CH_4 and CO in the first column and CO_2 , C_2H_4 , C_2H_6 and $\text{C}_3\text{H}_6/\text{C}_3\text{H}_8$ in the second column. In channel 1 the injector and oven temperatures were 70°C and 75°C , respectively while in channel 2 the temperatures for injector and column were 80°C and 70°C , respectively.

2.3.9 Mass, energy and carbon yields.

The biogas yield Y_{biogas} and digestate yield Y_{digest} was obtained from the evolved mass of biomass m_{biogas} and the input of feed to anaerobic digestion m_{ADfeed} to the digester:

$$Y_{\text{biogas}} = \frac{m_{\text{biogas}}}{m_{\text{ADfeed}}} \times 100; Y_{\text{digest}} = \frac{m_{\text{ADfeed}} - m_{\text{biogas}}}{m_{\text{ADfeed}}} \times 100$$

The yield in biochar and pyrolysis liquids were determined from initial mass of pyrolysis feed m_{PYfeed} and the recorded mass of biochar m_{biochar} and liquid phases m_{aq} , m_{org} :

$$Y_{\text{biochar}} = \frac{m_{\text{biochar}}}{m_{\text{PYfeed}}} \times 100; Y_{\text{aq}} = \frac{m_{\text{aq}}}{m_{\text{PYfeed}}} \times 100; Y_{\text{org}} = \frac{m_{\text{org}}}{m_{\text{PYfeed}}} \times 100$$

Biochar mass was recorded after pyrolysis. The phase-separated pyrolysis liquids were centrifuged (10000 g, 10 min), decanted

and the mass of both phases was recorded. The yield in non-condensable gases Y_{NCG} was obtained from:

$$Y_{\text{NCG}} = \frac{\sum_i m_{\text{NCG}_i}}{m_{\text{PYfeed}}} \times 100,$$

where m_{NCG_i} represents the mass of gaseous compound i , calculated from the measured volume and the ideal gas law. The energy yields E_Y were calculated from the HHV of the feedstock E_{FS} , the product E_i and its mass yield Y_i .

$$E_Y = \frac{E_i \times Y_i}{E_{\text{FS}}}$$

The feedstock denotes either raw cocoa/cocoa and manure for anaerobic digestion, or the digestate for pyrolysis. The carbon yield C_Y was similarly obtained from the feedstock's and product's carbon content C_i and the product's mass yield Y_i .

3 Results and discussion

3.1 Cocoa pod husks characteristics

The cocoa pod husks had a relatively high ash content of 11.38 wt.% (db) (Table 1), compared to other lignocellulosic agricultural residues like woody biomass⁴⁰. This ash fraction constitutes the nutrients withdrawn from soil, like alkali and alkaline earth metals, but also cadmium and lead, among others.

The European threshold for processing of cocoa beans to consumer goods is $0.60 \text{ mg} \cdot \text{kg}^{-1} \text{ Cd}$. The Cd concentration in the Manabí province (origin of used cocoa pod husks) typically ranged between $0.27 \text{ mg} \cdot \text{kg}^{-1}$ to $0.56 \text{ mg} \cdot \text{kg}^{-1}$ Argüello *et al.*⁴¹. The herein measured content of cadmium in cocoa pods was $0.314 \text{ mg} \cdot \text{kg}^{-1}$ and, according to Gramlich *et al.*⁴², similar concentrations in cocoa beans can be expected. Hence, the cocoa plantation from which the cocoa pod husks were derived, adhered to European regulations. The observed concentration of lead was *ca.*, 6 times smaller than that of cadmium (Table 1).

The observed volatile matter content and fixed carbon contents were 76.14 wt.% (daf) and 24.37 wt.% (daf), respectively. The volatile matter content of cocoa pod husks was lower than e.g., wood, in contrast to its fixed carbon content (for wood: VM daf: 84 wt.% and FC daf: 16 wt.%)⁴³. This indicates the increased tendency of cocoa pod husks for biochar formation upon pyrolysis.

The empirical chemical formula of the cocoa pod husks was derived from Table 1, being $\text{CH}_{1.4}\text{O}_{0.7}\text{N}_{0.03}$ and reflects its lignocellulosic nature. Carbohydrates and lignin constitute *ca.*, 46 wt.% and 15 wt.%²⁹, respectively. From their respective empirical chemical formulas $\text{CH}_{1.7}\text{O}_{0.8}$ and $\text{CH}_{1.1}\text{O}_{0.4}$ ⁴⁴, a theoretical empirical chemical formula of cocoa pod husk composition was obtained, being $\text{CH}_{1.5}\text{O}_{0.7}$. This is close to that derived from elemental analysis.

The HHV of cocoa pod husks was *ca.*, $16.49 \text{ MJ} \cdot \text{kg}^{-1}$, which is on the lower end of lignocellulosic biomasses (typically 18-19 $\text{MJ} \cdot \text{kg}^{-1}$)⁴⁵. This is likely due to the elevated ash content with no calorific value.

Table 1 Characterisation of the raw cocoa pod husks and resulting digestes from mono-digestion and co-digestion with cow manure. ar: as received; db: dry basis; daf: dry-and-ash-free basis; raw cocoa: undigested cocoa pod husks; mono-dig.: mono-digested cocoa pod husks; co-dig.: co-digested cocoa pod husks with cow manure

	Proximate analysis wt. %							Elemental analysis wt. %					Metals $\mu\text{g} \cdot \text{kg}^{-1}$		HHV $\text{MJ} \cdot \text{kg}^{-1}$	pH
	MC (ar)	VM (db)	VM (daf)	Ash (db)	FC (db)	FC (daf)	N (db)	C (db)	H (db)	O (db)	H/C	O/C	Cd	Pb	(db)	
Raw cocoa	3.80 ± 0.16	67.13 ± 0.27	76.14 ± 0.43	11.38 ± 0.25	21.49 ± 0.18	24.37 ± 0.22	1.38 ± 0.10	43.55 ± 0.37	5.18 ± 0.08	38.51 ± 0.39	1.43 ± 0.03	0.66 ± 0.01	314 -	54 -	16.49 ± 0.28	5.52 ± 0.02
Mono- dig.	9.09 ± 0.26	65.53 ± 0.33	80.91 ± 0.93	17.28 ± 0.68	17.19 ± 0.48	21.22 ± 0.63	1.20 ± 0.04	41.93 ± 0.44	5.24 ± 0.11	34.35 ± 0.37	1.50 ± 0.05	0.62 ± 0.01	1290 -	103 -	16.07 ± 0.12	9.92 ± 0.06
Co- dig.	11.43 ± 0.23	65.38 ± 0.17	77.07 ± 0.61	13.43 ± 0.48	21.19 ± 0.01	24.98 ± 0.11	2.19 ± 0.01	38.34 ± 0.43	4.72 ± 0.04	41.32 ± 0.45	1.48 ± 0.01	0.81 ± 0.02	1236 -	491 -	14.34 ± 1.60	8.96 ± 0.02

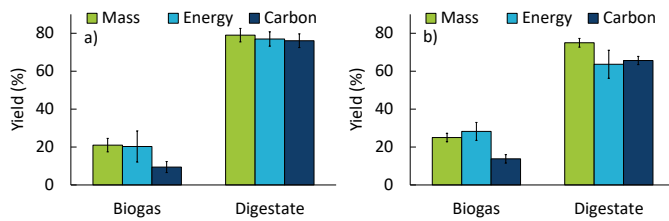
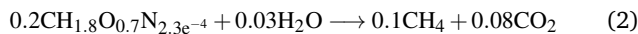
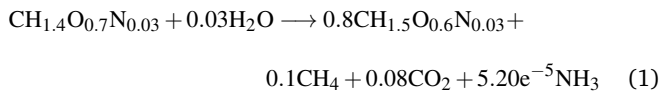


Fig. 2 Mass, energy and carbon yield of the products from anaerobic mono-digestion of cocoa pod husks (a) and anaerobic co-digestion of cocoa pod husks (b).

3.2 Anaerobic digestion of cocoa pods

3.2.1 Mono-digestion.

The yield in biogas was 21 ± 3.6 wt.% upon mono-digestion, leaving a digestate at a yield of 79 ± 3.6 wt.% (Fig. 2 a). The composition of the biogas was *ca.*, 54 ± 24 vol.% CH_4 and 46 ± 19 vol.% CO_2 . The digestate had an empirical chemical formula of $\text{CH}_{1.5}\text{O}_{0.6}\text{N}_{0.02}$ (from Table 1). Compared to cocoa pod husks, the O/C ratio of the mono-digestate decreased, while the H/C ratio increased (Table 1). This already suggests that oxygen-rich carbohydrates were digested more selectively than other biomass fractions, as hypothesized. A comprehensive impression on compositional changes induced by digestion was obtained from the schematic conversions below, derived from the Bushwell and Meuller relation⁴⁶:



Equations 1 and 2 were obtained by maximizing the elemental balance closure for each element, while minimizing the difference between the calculated and experimentally observed digestate yield and biogas composition. The balance for C, H, O and N were in Eq. 1 were 99.99%, 92.02%, 103.74% and 133.57%, respectively. The deviation for nitrogen was due to nitrogen in biogas (NH_3), of which the CG was not capable to detect it.

Equation 1 illustrates the conversion of cocoa pod husks to digestate and biogas, while Eq. 2 illustrates the conversion of the digestable fraction to biogas. This fraction $\text{CH}_{1.8}\text{O}_{0.7}\text{N}_{3\text{e}^{-4}}$ clearly re-

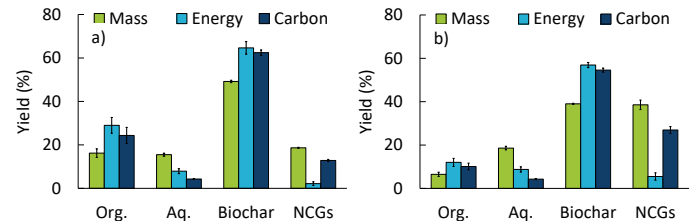


Fig. 3 Mass, energy and carbon yield of the products from slow pyrolysis of raw cocoa pod husks at 350 °C (a) and at 500 °C (b).

sembles carbohydrates in composition ($\text{CH}_{1.7}\text{O}_{0.8}$). It follows that the mass-loss upon mono-digestion, being 21 wt.%, constituted *ca.*, 50% of the available carbohydrate matrix²⁹. Antwi *et al.*²⁴ also observed a biodegradability index (*i.e.*, the observed biogas yield over theoretic biogas yield) between 41% to 47% (cellulose had a digestibility index of 84%). This indicates that the digestate will be lignin-enriched.

Fig. 2a shows that a significant fraction of mass carbon and energy is retained in the digestate. This carbon and energy retention, as well as the altered composition of the lignin-enriched mono-digestate, inevitably affected the pyrolysis product yields and composition of pyrolyzed mono-digestate, compared to fresh cocoa pod husks (Section 3.4).

3.2.2 Co-digestion with manure.

Compared to mono-digestion, co-digestion directed the distribution of mass, carbon and energy towards the biogas. Co-digestion resulted in an elevated biogas yield of 25 ± 2.3 wt.% (compared to 21 ± 3.6 wt.%). The methane content also increased to 60 vol.% CH_4 (compared to 54 vol.% CH_4 for mono-digestion. This was also reflected by the energy yield in the biogas (Fig. 2). The energy yield in biogas was 28.24 ± 4.74 %, being *ca.*, 8 percent points higher than for mono-digestion. The reason for this lies in the pH buffering capacity, as well as the effect of indigenous microorganisms in the cow-manure, among others. A detailed discussion on the effect of cow manure on biogas yield and composition is provided elsewhere⁴⁷.

The co-digestate was more carbon and energy deficient (Fig. 2 b). Typical ranges for C, H, N and O (wt.% db) in cow manure are 40.5-44.8 for C, 5.2-5.9 for H, 2.1-2.3 for N and 34.4-38.2 for O^{35,48,49}. The elevated nitrogen content in cow manure increased the nitrogen content of the digestate from co-digestion,

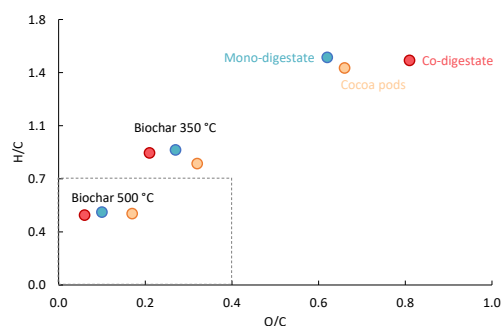


Fig. 4 van Krevelen diagram of fresh cocoa pod husks, digestates and their corresponding biochars.

being 2.19 ± 0.01 wt.% (db), compared to raw cocoa (1.38 ± 0.10 wt.%) and mono-digestate (1.20 ± 0.04 wt.%), see Table 1.

After anaerobic digestion in general, the quantity of solid cocoa residues decreased by 21-25 wt.%, while generating biogas with a calorific value between *ca.*, 16-19 MJ·kg⁻¹). The digestates still retained a lot of energy which typically is not valorised evidently. Land application of digestate does not fully make use of the digestate's potential and moreover requires additional hygienization measures. Incineration is on the other hand hampered by the high ash content of the cocoa pod husks and resulting digestates, which can cause slagging inside ovens. Therefore, the quantity and quality of evolved products from slow pyrolysis of raw cocoa pod husks were compared to those from anaerobic digestion and those from slow pyrolysis of the obtained digestates in an integrated approach.

3.3 Slow pyrolysis of cocoa pod husks

Biochar always was produced in the highest yield, being 49.20 ± 0.57 wt.% at 350 °C and 39.00 ± 0.28 wt.% for pyrolysis at 500 °C (Fig. 3). The fixed carbon contents (db) and (daf) of biochar were higher than those of the fresh cocoa pods (Table 2 and 1) and increased with the pyrolysis temperature, and this at the expense of the volatile matter content.

The carbon and energy yield in biochar from pyrolysis of raw cocoa pod husks is remarkable, as they both reach *ca.*, 63% for biochar produced at 350 °C and *ca.*, 55% if produced at 500 °C (Fig. 3). Although these biochar samples retained energy to a large extent, they also retained ash, which negatively impacts energy recovery *via* incineration. The ash recovery within both biochars was $69.08 \pm 7.55\%$ for biochar produced at 350 °C and $75.60 \pm 2.31\%$ for biochar produced at 500 °C. Nutrient reallocation upon field applications of both temperature biochars might therefore be more opportune, although biochar from 500 °C pyrolysis is more attractive from an elemental point-of-view. The van Krevelen diagram in Fig. 4 is annotated with the International Biochar Initiative (IBI) maximum threshold for H/C, being 0.7, and the European Biochar Certificate (EBC) maximum criteria for O/C, being 0.4. The highlighted area in Fig. 4 contains the biochars which meet these voluntary guidelines for high quality biochar, which were only those biochars obtained upon 500 °C pyrolysis.

The measured pH of the obtained biochar from both temperatures was approximately 9.50. From this, a decrease of Cd uptake by cocoa beans can be anticipated upon soil application. Argüello *et al.*⁴¹ showed that an increase of the soil pH by one unit, would result in a decrease of the Cd-uptake by a factor 1.6. Biochar application in Ecuadorian soil (typical pH 6⁴¹), can thus decrease the Cd concentration in cocoa pod beans. Moreover, biochar has been demonstrated to effectively adsorb both Cd and Pb⁵⁰.

The mass yield of the organic phase was 16.20 ± 1.98 wt.% (350 °C) and 6.50 ± 0.99 wt.% (500 °C) and lower than the biochar yield. The energy yield for both organic phases (28.99 ± 3.63 % for 350 °C; 12.02 ± 1.84 % for 500 °C) were larger than their mass yields, meaning that energy is concentrated in the organic phase (Fig. 3). This concentration of energy was in tandem with the concentration of carbon in the organic phase. The calculated HHV of the organic phases were 29.51 ± 0.64 and 30.49 ± 0.40 MJ·kg⁻¹ (for 350 °C and 500 °C, resp.), which was higher than their corresponding biochars (Table 2). The elemental composition of the organic phase is summarized in Table 3. The mass fraction of oxygen and nitrogen in the organic phase decreased, compared to the raw cocoa pod husks. This decrease was more pronounced for the organic phase obtained at 500 °C, compared to 350 °C. The GC-detectable fraction of the organic phase mainly contained (i) light oxygenates (4.39 ± 0.89 wt.% produced at 350 °C; 6.46 ± 2.39 wt.% produced at 500 °C), (ii) 2-cyclopenten-1-one derivatives (1.71 ± 0.34 wt.% produced at 350 °C and 3.63 ± 1.28 wt.% produced at 500 °C) and (iii) various phenolics (lumped concentration of 5.81 ± 0.21 wt.% if produced at 350 °C and 7.86 ± 1.24 wt.% if produced at 500 °C), see Fig. 6.

The aqueous phase was obtained with a yield of 15.50 ± 0.71 wt.% (350 °C) and 18.60 ± 0.85 wt.% (500 °C), see Fig. 3. Although the aqueous phase came in meaningful quantities, only minor quantity of carbon was retained in this fraction. The water content of the aqueous phase obtained at 350 °C amounted to 76.29 ± 2.44 wt.%, while that from the aqueous phase obtained at 500 °C was 79.76 ± 1.01 wt.%. The few carbon species within the aqueous phase, giving it a certain calorific value, were majorly light oxygenates, like acetic acid (Figure B1 in Supplementary Information).

The evolution of non-condensable gases from pyrolysis of cocoa pod husks showed a steep increase from 350 °C to 500 °C (Fig. 3). Especially for pyrolysis at 500 °C, the carbon yield in non-condensable gases was remarkable, being 38.65 ± 2.20 %. Nevertheless, the dominant compound in this stream was carbon dioxide, at a concentration of 77.78 ± 8.44 vol.% on N₂-free basis for pyrolysis at 350 °C and 79.51 ± 8.01 vol.% on N₂-free basis for pyrolysis at 500 °C. In the case of pyrolysis at 500 °C, CO, CH₄ and H₂ were also present at concentrations of 13.22 ± 6.87 vol.%, 3.94 ± 0.31 vol.% and 2.50 ± 0.92 vol.%, respectively. The resulting HHV of the non-condensable gases (N₂-free basis) from pyrolysis at 350 °C was 1.92 ± 0.74 MJ·kg⁻¹, while that from pyrolysis at 500 °C was 2.35 ± 0.70 MJ·kg⁻¹.

Overall, pyrolysis of raw cocoa pod husks mostly results in biochar, which can be used for soil applications, given the elevated pH (hence decreased Cd uptake), increased fixed carbon

Table 2 Characterisation of biochar samples obtained from slow pyrolysis of (i) raw cocoa pod husks, (ii) mono-digestate and (iii) co-digestate at 350 °C and 500 °C. ar: as received; db: dry basis; daf: dry-and-ash-free basis; raw cocoa: undigested cocoa pod husks; mono-dig.: mono-digested cocoa pod husks; co-dig.: co-digested cocoa pod husks with cow manure

	Proximate analysis wt. %							Elemental analysis wt. %					Metals $\mu\text{g} \cdot \text{kg}^{-1}$		HHV $\text{MJ} \cdot \text{kg}^{-1}$	pH
	MC (ar)	VM (db)	VM (daf)	Ash (db)	FC (db)	FC (daf)	N (db)	C (db)	H (db)	O (db)	H/C	O/C	Cd	Pb	(db)	
Cocoa	1.73	35.61	42.53	15.98	48.41	57.81	1.43	55.29	3.70	23.59	0.80	0.32	-	-	21.66	9.50
350 °C	± 0.45	± 1.00	± 1.51	± 1.70	± 2.70	± 3.46	± 0.05	± 0.77	± 0.06	± 2.31	± 0.01	± 0.04	-	-	± 0.86	± 0.02
Cocoa	0.10	20.18	25.90	22.06	57.76	74.13	1.02	60.94	2.39	13.59	0.47	0.17	48	100	24.06	9.56
500 °C	± 0.13	± 0.93	± 1.20	± 0.44	± 0.94	± 1.28	± 0.10	± 0.82	± 0.06	± 0.88	± 0.01	± 0.01	-	-	± 0.24	± 0.01
Mono-dig	1.08	35.99	48.23	25.11	38.76	51.95	1.94	51.00	3.77	18.19	0.89	0.27	-	-	22.34	12.21
350 °C	± 0.09	± 1.04	± 1.40	± 0.07	± 1.36	± 1.83	± 0.07	± 1.83	± 0.05	± 1.85	± 0.02	± 0.04	-	-	± 0.34	± 0.02
Mono-dig	0.00	18.43	27.32	32.54	49.03	72.68	1.54	56.34	2.28	7.30	0.48	0.10	899	1355	22.70	12.42
500 °C	± 0.00	± 0.25	± 0.38	± 0.19	± 0.23	± 0.40	± 0.04	± 2.09	± 0.15	± 2.19	± 0.01	± 0.03	-	-	± 0.05	± 0.01
Co-dig	0.67	39.96	48.19	23.14	39.91	52.03	1.65	55.58	4.00	15.63	0.87	0.21	-	-	23.19	10.24
350 °C	± 0.02	± 0.31	± 0.48	± 0.40	± 0.10	± 0.30	± 0.15	± 0.35	± 0.02	± 0.21	± 0.00	± 0.00	-	-	± 0.22	± 0.06
Co-dig	0.00	18.35	26.06	29.58	52.07	73.94	1.40	61.66	2.36	5.02	0.46	0.06	204	306	23.77	11.36
500 °C	± 0.00	± 0.07	± 0.11	± 0.13	± 0.20	± 0.32	± 0.14	± 1.61	± 0.03	± 1.53	± 0.01	± 0.02	-	-	± 0.17	± 0.01

Table 3 Characterisation of the organic phase obtained from slow pyrolysis of cocoa pod husks, mono-digestate and co-digestate

Org. Phase	N (db)	C (db)	H (db)	O (db)	H/C	O/C
Raw cocoa	3.79	63.16	8.28	24.76	1.57	0.29
350 °C	± 0.35	± 5.78	± 0.41	± 5.80	± 0.16	± 0.07
Raw cocoa	4.28	67.81	8.10	19.78	1.43	0.22
500 °C	± 0.09	± 0.67	± 0.15	± 0.78	± 0.03	± 0.01
Mono-dig.	3.95	52.48	9.17	33.99	2.10	0.49
350 °C	± 0.51	± 2.10	± 0.11	± 2.56	± 0.09	± 0.04
Mono-dig.	5.57	60.40	8.00	25.55	1.59	0.32
500 °C	± 1.29	± 11.15	± 0.94	± 13.15	± 0.35	± 0.17
Co-dig.	4.46	69.50	8.65	16.99	1.49	0.18
350 °C	± 0.19	± 1.10	± 0.07	± 0.89	± 0.03	± 0.01
Co-dig	5.74	64.31	8.37	21.38	1.56	0.25
500 °C	± 0.28	± 4.93	± 0.45	± 4.64	± 0.15	± 0.06

content for carbon sequestration and the re-allocation of nutrients. The organic phases from pyrolysis were very carbon and energy dense (having a HHV of *ca.*, 28-30 $\text{MJ} \cdot \text{kg}^{-1}$) and contained mostly light oxygenated compounds and phenolics. The non-condensable gases mostly consisted of CO_2 .

3.4 Integrated slow pyrolysis of digested cocoa pod husks

The average mass balance closure of the two digestates at two different temperatures, each in duplicate, was $97.3 \pm 6.7\%$ (Fig. 5 and 7). It should be noted that the mass balance closures from pyrolysis experiments with co-digestate were considerably lower than those of the other experiments (91.90 ± 3.62 for 350 °C and 95.81 ± 7.18 for 500 °C). This was presumed to be NH_3 , which evolved during slow pyrolysis and which the micro-GC was not capable to detect and quantify. During the recovery of pyrolysis liquids after the experiments, the specific odor of ammonia was indeed recognised.

3.4.1 mono-digestion coupled to slow pyrolysis.

Pyrolysis at 350 °C overall resulted in similar mass, energy and carbon distributions over the different pyrolysis products, compared to pyrolysis of raw cocoa pod husks at the same temperature. At a pyrolysis temperature of 500 °C, an increase of the

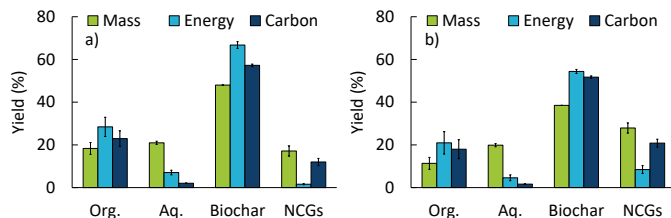


Fig. 5 Mass, energy and carbon yield of the products from slow pyrolysis of mono-digested cocoa pod husks at 350 °C (a) and at 500 °C (b)

organic phase by *ca.*, 5 percent points was notable, at the expense of non-condensable gases. This was ascribed to alterations in the biocomposition of the cocoa pod husks, induced by the digestion process itself (*i.e.*, having a hydrolysis step). Anaerobic digestion resulted in a digestate more prone to volatilisation into pyrolysis liquids and non-condensable gases, as evidenced by the higher VM content of digestate (Table 1). The increase of pyrolysis liquids at the expense of non-condensable gases from pyrolysis of mono-digestate at 500 °C is then explained by the origin of the volatile fraction. The lignin-enriched digestate resulted in pyrolysis vapors, that are typically less prone to consecutive cracking to *e.g.*, CO_2 and CO . The typical precursor for suchlike gases upon pyrolysis at 500 °C is the holocellulose fraction⁵¹, which was partly digested prior to pyrolysis (Section 3.2.1).

Differences in the product properties also were apparent. The ash content of biochar derived from the mono-digestate at 350 °C and 500 °C was 10 percent points higher than in their undigested counterparts (Table 2). This was because ash already was retained in the mono-digestate, resulting in an ash-enriched mono-digestate, prior to pyrolysis. The ash recoveries throughout the coupled digestion-pyrolysis process were $83.66 \pm \%$ (for 350 °C) and $86.97 \pm 4.41\%$ (for 500 °C).

Like undigested cocoa pods, only biochar from mono-digestate produced at 500 °C complied with IBI and EBC guidelines (Fig. 4). The O/C ratio decreased however remarkably from 0.32 (raw cocoa pod husks at 350 °C, Table 2) to 0.27 (mono digestion at 350 °C, Table 2). On the other hand, the H/C ratio in-

creased from 0.80 (raw cocoa pod husks, 350 °C) to 0.89 (mono-digestate, 350 °C). Biochar obtained at 500 °C, before and after mono-digestion, only changed in terms of the O/C ratio. The O/C ratio dropped from 0.17 for biochar from fresh cocoa pod husks, to 0.10 for biochar from mono-digestate. Moreover, mono-digestate derived biochar showed very high pH values of *ca.* 12 (Table 2), indicating a high potential to decrease Cd uptake in cocoa beans from soil⁴¹.

The fixed carbon content (db and daf) was however lower for biochars obtained from mono-digestate at the same temperature, compared to biochar obtained from fresh cocoa pod husks. Typically, the fixed carbon content increases with decreasing O/C ratios⁵², which was not the case here (Table 2). The same reason was put forth used to explain the increased volatile matter content of the mono-digestate compared to the raw cocoa pods. The hydrolysis step during anaerobic digestion could have altered the biomass' structure, making it more prone to volatilisation, hence less prone to solids formation. Biochar that results from digestate is then also expected to have a lower fixed carbon content than the biochar from the unaltered (*i.e.*, undigested) cocoa pod husks.

The pyrolysis liquids from mono-digestate obtained at 350 °C contained virtually no light oxygenates anymore, compared to direct pyrolysis of cocoa pod husks (Fig. 6 and Figure C2 in Supplementary Information). The holocellulose-derived 2-cyclopenten-1-one derivatives in the organic phases obtained from pyrolysis of mono-digestate at 350 °C (1.24 ± 0.06 wt.%) and 500 °C (1.40 ± 0.08 wt.%) were lower than the organic phase from pyrolysis of raw cocoa pod husks (1.71 ± 0.34 wt.% obtained at 350 and 3.63 ± 1.28 wt.% obtained at 500 °C). These results further confirm that the mono-digestate became lignin-enriched, as mainly carbohydrates were digested into biogas. The fact that 2-cyclopenten-1-one derivatives merely increased in the organic phase between pyrolysis at 500 °C and pyrolysis at 350 °C suggests that a significant fraction of the cellulose was already digested. Indeed, pyrolysis at 350 °C will typically volatilise only a fraction of the cellulose, as the decomposition of cellulose (apparent from thermogravimetric analysis) occurs between 320 to 420 °C⁵³. The fact that no additional 2-cyclopenten-1-one derivatives evolved after pyrolysis at 500 °C reflects the smaller contribution of cellulose in the mono-digestate (compared to cocoa pod husks) that would decompose beyond 350 °C.

The main GC-detectable constituents in the organic phase were phenolics at similar concentrations as the organic phase from undigested cocoa pod husks: 6.10 ± 0.11 wt.% for the mono-digestate derived organic phase at 350 °C and 5.81 ± 0.40 wt.% for the raw cocoa pod husk-derived organic phase at 350 °C (Fig. 6). For pyrolysis at 500 °C, again a similar total quantity of phenolics was obtained. Nevertheless, the composition of the "phenolics pool" changed. While pyrolysis at 500 °C resulted in less methoxyphenols (2-methoxyphenol, or guaiacol, and 2,6-dimethoxyphenol, or syringol) and methoxyalkylphenols (2-methoxy-4-ethylphenol, 2-methoxy-4-methylphenol), more alkylphenols (methylphenol and ethylphenol) and phenol were observed, see Fig. 6 and Figure C2 in Supplementary Information. This is due to temperature-induced demethoxylation and dealkylation reactions, being more

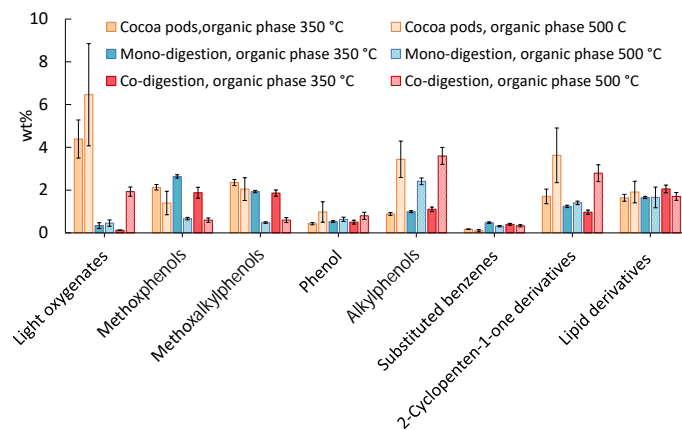


Fig. 6 Composition of the organic phase pyrolysis liquids in wt.% on liquid-basis from pyrolysis of raw cocoa, mono-digested cocoa and co-digested cocoa at 350 °C and 500 °C, determined through GC-MS analysis.

pronounced at 500 °C.

These phenolics present extra value, as these can be (selectively) extracted to recover specific compounds, like 2-methoxy-4-ethylphenol and 2-methoxyphenol⁵⁴. Alternatively, the organic phase can be used to recover energy, given its calorific value of 24.92 ± 1.02 MJ·kg⁻¹ (from pyrolysis at 350 °C) and 29.69 ± 1.31 MJ·kg⁻¹ (from pyrolysis at 500 °C). The higher calorific value of the organic phase from pyrolysis of mono-digestate at 500 °C was due to the elevated presence of alkylphenols and reduced presence oxygenated aromatics, respectively (Fig. 6 and Figure C2 in Supplementary Information).

The nitrogen content of the organic phase was 3.95 ± 0.51 wt.% (obtained at 350 °C) and 5.75 ± 1.29 wt.% (obtained at 500 °C), Table 3. The nitrogen content in the organic phase from mono-digestate pyrolysis at 500 °C was visibly higher than that from raw cocoa pod pyrolysis at 500 °C (4.28 ± 0.09 wt.%). Since only traces of nitrogen-containing compounds were GC-detectable (*e.g.*, indole in Fig. C2, Supplementary Information), nitrogen was assumed to be present in the high molecular weight fraction of the organic phase. The organic phases from slow pyrolysis of mono-digestate also contained more oxygen by mass: *ca.* 20-25 wt.% for raw cocoa pod husks and *ca.* 26-34 wt.% for mono-digestate. Fig. 6 does not point out any specific oxygen-containing constituents (or group of compounds) among the GC-detectable compounds at an elevated concentration to explain the increased oxygen content. Hence, the additionally measured oxygen in the organic phase would be present in the heavy fraction as well, not detectable by GC-MS analysis. As stated earlier, anaerobic digestion (and its associated hydrolysis) could have altered the cocoa pod husks' structure in such way that the mono-digestate was more prone to yield pyrolysis liquids, rather than biochar. Thus, oxygen-containing fractions of the cocoa pod husks that would result in solid biochar (if undigested), ended up in heavy organic phase liquids due to prior anaerobic digestion. Table 3 and 2 indeed show that, while the oxygen content of biochar decreased upon prior digestion, the oxygen content of the organic

phase increased.

Regarding the non-condensable gases, a decrease in the yield (especially upon pyrolysis at 500 °C) was observed, but the average composition of the non-condensable gases remained quasi the same. From pyrolysis at 350 °C of undigested cocoa pods and mono-digestate, the gas volumetric composition was 1:0.27:0:0 and 1:0.20:0:0 CO₂:CO:H₂:CH₄ vol.%, respectively. Pyrolysis of the undigested cocoa pod husks and mono-digestate at 500 °C resulted in 1:0.24:0.05:0.05 CO₂:CO:H₂:CH₄ vol.% and 1:0.20:0.17:0.11, respectively. Pyrolysis at 350 °C thus resulted in CO₂ and CO only, whereas pyrolysis at 500 °C resulted in an evolution of hydrogen gas (which was modestly more pronounced for pyrolysis of mono-digestate). Hydrogen evolution at elevated temperatures is due to aromatization, in which polyaromatic centres within the biochar are being formed and H₂ is being ejected. Because the rather low contribution of CO and H₂ in the off-gases from pyrolysis, this stream bears little energy: 1.47 ± 0.12 MJ · kg⁻¹ (N₂-free) for pyrolysis at 350 °C. Although still low, the HHV of non-condensable gases from pyrolysis of mono-digestate at 500 °C doubled (4.78 ± 0.96 MJ · kg⁻¹), compared to raw cocoa pod husks at the same temperature.

Overall, mono-digestion did result in a digestate that is more favorable for subsequent slow pyrolysis. While the product yields between raw cocoa pod husks and its mono-digestate after pyrolysis at 350 °C did merely change, the obtained organic phase from mono-digestate was poor in carbohydrate-derived compounds. This is advantageous in two ways: (i) the composition of the organic phase became more homogeneous, meaning that phenolic compounds were concentrated as useful biorefinery intermediates (*vide infra*) and (ii) the chemical energy within the carbohydrate fraction was released in the form of biogas as easy and readily available energy source upon anaerobic digestion. Indeed, carbohydrate-derived compounds like light oxygenates in the organic phase are not easily recovered for further utilization. After pyrolysis at 500 °C, biochar from mono-digestate was obtained at the same yield, yet being more de-oxygenated than biochar from raw cocoa pod husks. The resulting biochar moreover had a higher pH, beneficial to soil applications.

3.4.2 co-digestion coupled to slow pyrolysis.

Upon slow pyrolysis of co-digestate more aqueous phase pyrolysis liquids were obtained (between *ca.*, 23 to 25 wt.%), compared to undigested cocoa pods after pyrolysis at the same temperature (between *ca.*, 16 to 19 wt.%). In contrast, little organic phase was obtained for co-digestate pyrolysis at both temperatures (*ca.*, 5 wt.%, Fig. 7), compared to pyrolysis of mono-digestate (*ca.*, 11-18 wt.%, Fig. 5) and raw cocoa pod husks (*ca.*, 7-16 wt.%, Fig. 3).

Application of co-digestate resulted in biochar that shared similar properties with mono-digestate derived biochars. The fixed carbon content, volatile matter content, calorific value, the H/C and O/C ratio were similar for same-temperature biochars. Hence, data points for these biochars were in close proximity to those for mono-digestate derived biochar in Fig. 4. This similarity is remarkable, considering the difference in nitrogen content of the starting materials for pyrolysis in Table 1. The additional

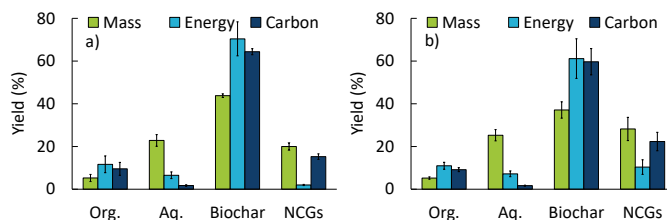


Fig. 7 Mass, energy and carbon yield of the products from slow pyrolysis of co-digested cocoa pod husks at 350 °C (a) and at 500 °C (b)

nitrogen present in the co-digestate due to the cow manure thus was not entirely retained in the solid phase. Instead, nitrogen was reasonably assumed to have end up in the non-condensable gas stream as NH₃ (not in the pyrolysis liquids, *vide infra*), also causing a small deviation in the mass balance closure of the pyrolysis process with co-digestate.

The GC-detectable compounds of the pyrolysis liquids indicated that, upon co-digestion with cow-manure, less carbohydrates were converted into biogas, compared to mono-digestion. This was apparent from the increased contribution of light oxygenates, like acetic acid and 2-cyclopenten-1-one derivatives in the pyrolysis liquids (Fig. 6 and Fig. C2 in Supplementary Information). Pyrolysis of residual cellulose at 500 °C in the co-digestate should go in tandem with elevated concentrations of light oxygenates and 2-cyclopenten-1-one derivatives in the pyrolysis liquids, compared to pyrolysis at 350 °C (like for undigested cocoa in Fig. 6). Not observing this trend implies that more residual cellulose was present in the co-digestate, compared to the mono-digestate. Cow manure moreover does typically not contain more residual carbohydrates than the cocoa pod husks⁵⁵. These two observations indicate manure was more easily anaerobically digested than raw cocoa pod husks.

The nitrogen content of the organic phase from slow pyrolysis of co-digestate was only modestly higher (4.46 ± 0.19 wt.% for 350 °C and 5.47 ± 0.28 wt.%) than for the mono-digestate, despite the feedstock's elevated nitrogen content. This also supports the hypothesis that nitrogen in the co-digestate partitioned to the gas phase as NH₃. The calorific value of the obtained pyrolysis liquids' organic phase were 31.95 ± 0.44 MJ · kg⁻¹ (obtained at 350 °C) and 30.31 ± 0.12 MJ · kg⁻¹ (obtained at 500 °C), which is approximately as high as from raw cocoa pod husks. Both the high HHV and low nitrogen content make energy recovery for this stream very opportune.

The detected non-condensable gases were also rich in CO₂, followed by CO and H₂. The volumetric composition was 1:0.20:0:0 CO₂:CO:H₂:CH₄ vol.% (for 350 °C) and 1:0.19:0.11:0.12 CO₂:CO:H₂:CH₄ vol.% (for 500 °C). The contribution of CO and H₂ in the gas stream was smaller, compared to the mono-digestate. The average calorific value of the N₂-free gas stream from pyrolysis at 350 °C was along the lines of the other equivalent gas streams (1.43 ± 0.12 MJ · kg⁻¹), while that from pyrolysis at 500 °C was the highest one observed, being 5.30 ± 0.28 MJ · kg⁻¹.

Overall, co-digestion resulted in a digestate that in particular led to a better biochar, compared to undigested cocoa pods.

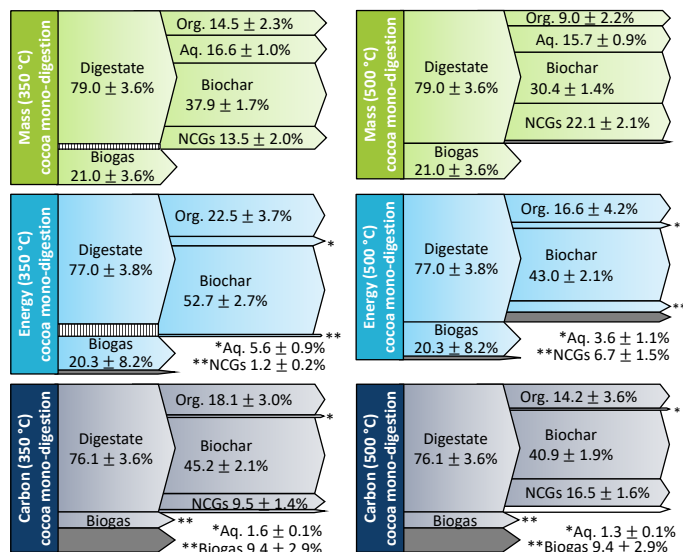


Fig. 8 Sankey diagrams for mass, energy and carbon of the integrated mono-digestion/slow pyrolysis process at pyrolysis temperatures of 350 °C and 500 °C. The dashed streams are errors, while the filled gray streams are losses.

Biochar from both temperatures were the most de-oxygenated among the other same-temperature biochars. The lowest H/C and O/C ratio among all biochars were also observed for biochar from this feedstock at 500 °C.

3.5 Overall process evaluation and biorefinery opportunities

Considering the comprehensive product portfolio of the studied processes, possible strategies are put forth and evaluated in this section to obtain maximum value from the starting cocoa pod husks. Value in its broadest meaning can be generated from (i) biochar applications in which nutrients are recycled and carbon is sequestered upon biochar soil amendment, among other applications^{56–58}, (ii) chemicals (especially phenolics) in the pyrolysis liquids' organic phase and (iii) energy from combustion of biogas, non-condensable gases, biochar and the organic phase pyrolysis liquids. Of lower interest is the aqueous phase of pyrolysis liquids, as it is in essence a very diluted acetic acid solution.

As principal constraint, it was put forth that candidate strategies for cocoa waste management should be self-sustaining in terms of energy. Slow pyrolysis requires significant energy input, which typically ranges between 6% to 15% of the pyrolysis feedstock energy content⁵⁹. This energy can be met by combustion of the non-condensable gases, depending on the feedstock and applied pyrolysis temperature⁵⁹. Table 4 presents energy yields relative to the pyrolysis feedstock energy content. From that table, it is clear that the non-condensable gases themselves bear insufficient energy (< 15%) to sustain the pyrolysis process, despite pyrolysis of plain cocoa pod husks results in the highest obtained quantities of biochar (49.20 ± 0.57 wt.%), carbon in biochar (62.46 ± 1.24 wt.%) and organic phase (16.20 ± 1.69 wt.%) with phenolics (0.94 ± 0.12 wt.%). Compensation for the lack of energy in the non-condensable gases by combustion of

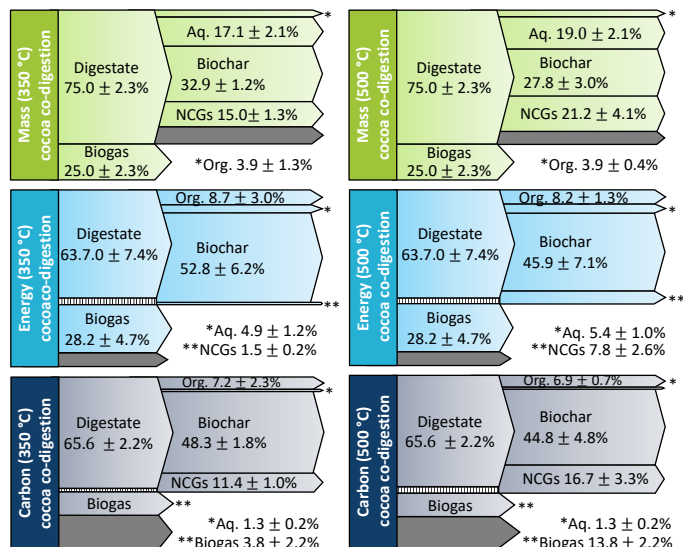


Fig. 9 Sankey diagrams for mass, energy and carbon of the integrated co-digestion/slow pyrolysis process at pyrolysis temperatures of 350 °C and 500 °C. The dashed streams are errors, while the filled gray streams are losses.

biochar and/or liquid products is considerable, but should however be avoided, as biochar and the organic phase themselves present value and biochar its elevated ash content can cause slagging during incineration for energy.

Once anaerobic digestion is coupled to slow pyrolysis, sufficient energy is available in the biogas and non-condensable gases (gas streams in Table 4) to sustain slow pyrolysis and recover additional energy. The energy in the gas streams (*ca.*, 30% for mono-digestion and 50% for co-digestion) always well-exceeded the upper limit of the required energy for pyrolysis, being 15%. There is even sufficient energy to additionally consume 2-5 MJ · kg⁻¹ to pre-dry the cocoa waste to a moisture content of 10 wt.%^{60,61}. Depending on the market situation, the product portfolio could be skewed towards either (i) energy and high quality biochar or (ii) energy/biochar and high quality organic phase oil.

In scenario (i), the output of energy and high quality biochar occurs through mono-digestion/slow pyrolysis at 500 °C and co-digestion/slow pyrolysis at 500 °C (Fig. 8 and 9). For co-digestion at 500 °C, 36% of the energy in cocoa pod husks/cow manure mixture was retained in the gas stream (28.2% in biogas, 7.8% in non-condensable gases, Fig. 9). Expressed on a co-digestate basis, this corresponds to *ca.*, 54.4% (Table 4), which is well above the maximum threshold of 15% put forth by Crombie and Mašek⁵⁹. For slow pyrolysis of mono-digestate at 500 °C, 34.81% of energy was present in the gas stream, relative to the digestate. This is also well above the required 15%. Biochar from co-digestion at 500 °C had the lowest H/C and O/C ratio (Fig. 4), indicating a high recalcitrance upon soil amendment (Table 2). Although this biochar thus presents the best quality in terms of O/C and H/C ratio, it also comes with the lowest mass and carbon yield of all processes (Fig. 9). A small increase in biochar yield (from 27.83 to 30.42 wt.%) can be expected if produced from mono-digestate at 500 °C. This biochar also complies to the IBI and

Table 4 Comparison of all pyrolysis and integrated processes by (i) the energy yield relative to the ^apyrolysis feedstocks (i.e., raw cocoa pods, mono-digestate and co-digestate) or to the ^braw feedstock (i.e., raw cocoa for direct pyrolysis, raw cocoa for mono-digestion and cocoa plus manure for co-digestion), (ii) mass yield relative to the raw feedstocks, (iii) carbon yield relative to the raw feedstocks and (iv) the phenolics yields relative to the raw feedstocks. ^cGas stream that only contains non-condensable gases.

	Product	Energy yield	^b Mass yield	Phenolics yield (%)
Raw cocoa 350 °C	^c Gas streams	^a 11.64 ± 4.51	18.64 ± 0.25	
	Biochar	64.64 ± 2.89	49.20 ± 0.57	
	Org. Phase	28.99 ± 3.63	16.20 ± 1.98	0.94 ± 0.12
Raw cocoa 500 °C	Gas streams	^a 14.24 ± 4.24	38.56 ± 2.20	
	Biochar	56.90 ± 1.19	39.00 ± 0.28	
	Org. Phase	12.02 ± 1.85	6.50 ± 0.99	0.38 ± 0.08
Mono-dig. 350 °C	Gas streams	^a 27.92 ± 10.70	34.53 ± 4.09	
	Biochar	52.73 ± 2.68	37.92 ± 1.71	
	Org. Phase	22.46 ± 3.70	14.48 ± 2.29	0.88 ± 0.11
Mono-dig. 500 °C	Gas streams	^a 34.81 ± 10.83	43.05 ± 4.16	
	Biochar	42.96 ± 2.08	30.42 ± 1.38	
	Org. Phase	16.56 ± 4.20	8.97 ± 2.24	0.55 ± 0.07
Co-dig. 350 °C	Gas streams	^a 46.07 ± 10.53	40.00 ± 2.65	
	Biochar	52.79 ± 6.18	32.85 ± 0	
	Org. Phase	8.74 ± 2.95	3.95 ± 1.26	0.21 ± 0.03
Co-dig. 500 °C	Gas streams	^a 54.44 ± 10.88	46.16 ± 4.73	
	Biochar	45.86 ± 7.09	27.83 ± 2.99	
	Org. Phase	8.24 ± 1.25	3.92 ± 0.41	0.22 ± 0.03

EBC guidelines (Fig. 4).

Whether or not mono- or co-digestate was opted as pyrolysis feedstock, additional energy could be gained by combustion of the organic phase. This appears advantageous when using co-digestate, because this organic phase yielded the least amount of valuable phenolics, relative to the cocoa and cow manure mixture. Moreover, the organic phase from this process also was very energy dense (ca., 2 times that of the cocoa/cow manure mixture) and contained few oxygen, compared to other organic phases. The nitrogen content also was only modestly higher, despite the elevated nitrogen content of the co-digestate. Nevertheless, appropriate pre- or post-treatment measures can be implemented to control the nitrogen content of the organic phase. Co-combustion of this organic phase would add 8.2 percent points to result in a total energy recovery of 57.6%, relative to the cocoa and cow manure mixture. In case of mono-digestate pyrolysis at 500 °C, 9.0 percent points would be added to obtain a total energy recovery from the gas stream and organic phase of 52.2%, relative to the digestate. This recovery is slightly lower than for co-digestate pyrolysis at 500 °C. Moreover, valuable phenolics in this organic phase (here, the highest among all organic phases produced at 500 °C) would remain poorly valorised. Therefore, the recovery of alkylphenols could be performed, along biochar and energy.

In scenario (ii), the output of energy/biochar and high quality organic phase oil occurs through mono-digestion/slow pyrolysis at 350 °C (Fig. 8, Table 4). Indeed, this integrated process recovers (more than) enough energy (27.92 ± 10.70 % on mono-digestate basis) to sustain pyrolysis. Moreover, the least amount of the less-valuable aqueous pyrolysis liquids among all processes were obtained (Fig. 8). On the other hand, Table 4 shows that the quantity of phenolics in the organic phase from pyrolysis of mono-digestate at 350 °C (0.88 ± 0.11 wt.%) is almost as high as for undigested cocoa pods (0.94 ± 0.12 wt.%), despite 21 wt.% of the cocoa pod husks was channeled to biogas (Fig. 8). This once more exemplifies that selectively converting the holocellu-

lose fraction in cocoa pod husks to biogas results in a lignin-enriched digestate from which phenolics could be obtained in almost similar quantities as direct pyrolysis. The phenolic compounds were mostly methoxyphenols and methoxyalkylphenols (Fig. 6). Therefore, extraction of these methoxy(alkyl)phenols might be opportune, as these are considered renewable building blocks for chemistry and plastic industry⁶²⁻⁶⁶. Recently, an extraction scheme has been proposed, able to separate these methoxyphenols with an increased selectivity, by carefully controlling the pH of the extracted solution⁵⁴. Alternatively, it has been suggested that the pooled group of phenolics could be valorised (with or without upgrading) to polyols and polyurethane foams, as well aromatics for fuel additives^{65,67}. After separating phenolics, meaningful quantities of the heavy organic phase remain, which can be used for energy recovery or as constituent for bio-asphalt or bio-bitumen⁶⁸. As ca., 16 wt.% of the organic phase was GC-detectable, the organic residue upon extraction of the GC-detectable fraction containing phenolics could be estimated to ca., 84 wt.%.

Biochar from scenario (ii) came in the highest relative yield (37.9 wt.%) among all four integrated processes, while also having the highest pH (hence, causing decreased Cd uptake by cocoa beans). Also, the O/C and H/C ratio of that biochar strongly decreased, but however not sufficient to fall in the range to adhere to the IBI and EBC voluntary guidelines (Fig. 4). Hence, the soil stability of this biochar will be lower than biochar from 500 °C of the same feedstock. Therefore, along with soil amendment for nutrient recovery, incineration can be considered, resulting in an energy recovery of 72.5% (20.3 from biogas and 52.7 from biochar, Fig. 8). However, the ash content has to be considered in this scenario.

4 Conclusions

This study demonstrated integrated anaerobic digestion/slow pyrolysis for agricultural residues, with cocoa pod husks as example

case. The integrated anaerobic digestion/slow pyrolysis process converted the biodegradable carbohydrates of the bio-waste into biogas, while converting the digestate with beneficial properties for subsequent processing through slow pyrolysis into superior biochar and pyrolysis liquids. By doing so, these voluminous cocoa pod husks can effectively be valorised into energy and valuable biorefinery intermediates, being biochar for soil amendment (and decreased Cd uptake) and organic liquids rich in phenolics for further upgrading. Biochar itself is recommended to be produced from the integrated co-digestion/slow pyrolysis process at 500 °C or from the integrated mono-digestion/slow pyrolysis process at 500 °C. Such strategies result in high quality biochar, with O/C ratios between 0.06 and 0.10, H/C ratios between 0.46 and 0.48 and a pH between 11.36 and 12.42. In both strategies, slow pyrolysis can be self sustaining and 52.2 and 57.6% of the energy could be recovered, relative to the initial mass of cocoa or cocoa plus manure. Alternatively, biochar could be obtained in higher yields and with higher pH upon mono-digestion/slow pyrolysis at 350 °C, however with O/C ratio of 0.27 and H/C ratio of 0.89. In this strategy, co-evolution of an organic phase rich in valuable phenolics (6.1 wt.% on liquid basis; 0.88 wt.% on feed-stock basis), especially methoxyphenols is realised. Overall, this study outlines the first essential steps towards the bio-refining of agricultural residues and cocoa pod waste into a valuable set of outgoing products.

Appendix A. Supplementary information

Supplementary information associated with this article can be found, in the online version, at doi.

Conflicts of interest

There are no conflicts to declare.

Acknowledgements

This work was supported by the project grant SENESCYT Convocatoria Abierta 2014 Primera Fase. Jo De Vrieze is supported as postdoctoral research fellow by the Research Foundation Flanders (FWO-Vlaanderen). We thank Amanda Luther for useful suggestions.

Notes and references

- 1 A. S. Matharu, J. A. Houghton, C. Lucas-Torres and A. Moreno, *Green Chem.*, 2016, **18**, 5280–5287.
- 2 A. Schievano, F. Adani, L. Buessing, A. Botto, E. N. Casoliba, M. Rossoni and J. L. Goldfarb, *Green Chem.*, 2015, **17**, 2874–2887.
- 3 L. Wang, J. G. Wang, J. Littlewood and H. B. Cheng, *Green Chem.*, 2014, **16**, 1527–1533.
- 4 F. Valenti, Y. Zhong, M. Sun, S. M. Porto, A. Toscano, B. E. Dale, F. Sibilla and W. Liao, *Waste Manage.*, 2018, **78**, 151–157.
- 5 L. T. Angenent, J. G. Usack, J. Xu, D. Hafenbradl, R. Posmanik and J. W. Tester, *Bioresource Technol.*, 2018, **247**, 1085–1094.
- 6 J. H. Clark, *Green Chem.*, 2019, **21**, 1168–1170.
- 7 S. Wang, W. Gao, L.-P. Xiao, J. Shi, R.-C. Sun and G. Song, *Sustainable Energy Fuels*, 2019, **3**, 401–408.
- 8 P. Choudhary, A. Malik and K. K. Pant, *Sustainable Energy Fuels*, 2020, **4**, 1481–1495.
- 9 D. C. Kalyani, T. Fakin, S. J. Horn and R. Tschentscher, *Green Chem.*, 2017, **19**, 3302–3312.
- 10 M. De bruyn, J. Fan, V. L. Budarin, D. J. Macquarrie, L. D. Gomez, R. Simister, T. J. Farmer, W. D. Raverty, S. J. McQueen-Mason and J. H. Clark, *Energy Environ. Sci.*, 2016, **9**, 2571–2574.
- 11 S. Ghysels, F. Ronsse, D. Dickinson and W. Prins, *Biomass Bioenerg.*, 2019, **122**, 349–360.
- 12 N. T. Farrokh, H. Suopajarvi, O. Mattila, K. Umeki, A. Phounglamcheik, H. Romar, P. Sulasalmi and T. Fabritius, *Energy*, 2018, **164**, 112–123.
- 13 Q. Feng and Y. Lin, *Renew. Sust. Energ. Rev.*, 2017, **77**, 1272–1287.
- 14 F. Monlau, C. Sambusiti, N. Antoniou, A. Barakat and A. Zabanitotou, *Applied Energy*, 2015, **148**, 32–38.
- 15 P. Smith, *Glob. Change. Biol.*, 2016, **22**, 1315–1324.
- 16 S. Gillet, M. Aguedo, L. Petitjean, A. R. C. Morais, A. M. da Costa Lopes, R. M. Łukasik and P. T. Anastas, *Green Chem.*, 2017, **19**, 4200–4233.
- 17 B. Satari, K. Karimi and R. Kumar, *Sustainable Energy Fuels*, 2019, **3**, 11–62.
- 18 ICCO, *International Cocoa Organization*, https://www.icco.org/about-us/international-cocoa-agreements/cat_view/30-related-documents/46-statistics-production.html, 2019, Accessed: 2019-11-28.
- 19 K. P. Nair, *The Agronomy and Economy of Important Tree Crops of the Developing World*, Elsevier, London, 2010, pp. 131–180.
- 20 Z. S. Vásquez, D. P. de Carvalho Neto, G. V. Pereira, L. P. Vandenberghe, P. Z. de Oliveira, P. B. Tiburcio, H. L. Rogez, A. G. Neto and C. R. Soccol, *Waste Manage.*, 2019, **90**, 72–83.
- 21 D. Guest, *Phytopathology*, 2007, **97**, 1650–1653.
- 22 M. Syamsiro, H. Saptoadi, B. Tambunan and N. Pambudi, *Energy Sustain. Dev.*, 2012, **16**, 74–77.
- 23 C. M. A. Fontes, R. B. Silva and P. R. L. Lima, *Waste Biomass Valori.*, 2019, **10**, 223–233.
- 24 E. Antwi, N. Engler, M. Nelles and A. Schüch, *Waste Manage.*, 2019, **88**, 131–140.
- 25 S. Dahunsi, C. Osueke, T. Olayanju and A. Lawal, *Bioresource Technol.*, 2019, **283**, 229–241.
- 26 N. Acosta, J. D. Vrieze, V. Sandoval, D. Sinche, I. Wierinck and K. Rabaey, *Bioresource Technol.*, 2018, **265**, 568–572.
- 27 J. K. Ogunjobi and L. Lajide, *Int. J. Green Energy*, 2015, **12**, 440–445.
- 28 M. Adjin-Tetteh, N. Asiedu, D. Dodoo-Arhin, A. Karam and P. N. Amaniampong, *Ind. Crop. Prod.*, 2018, **119**, 304–312.
- 29 D. Mansur, T. Tago, T. Masuda and H. Abimanyu, *Biomass Bioenerg.*, 2014, **66**, 275–285.

- 30 J. O. Titiloye, M. S. A. Bakar and T. E. Odetoeye, *Ind. Crop. Prod.*, 2013, **47**, 199 – 203.
- 31 C.-H. Tsai, W.-T. Tsai, S.-C. Liu and Y.-Q. Lin, *Biomass Conv. Bioref.*, 2018, **8**, 237–243.
- 32 O. Mašek, F. Ronsse and D. Dickinson, *Biochar in European soils and agriculture: science and practice*, Routledge, 2016, pp. 17–40.
- 33 G. Yildiz, M. Pronk, M. Djokic, K. M. van Geem, F. Ronsse, R. van Duren and W. Prins, *J. Anal. Appl. Pyrol.*, 2013, **103**, 343 – 351.
- 34 A. Enders and J. Lehmann, *Biochar: A Guide to Analytical Methods*, CRC press, 2017, pp. 9–22.
- 35 L. Young and C. C. Pian, *Energy*, 2003, **28**, 655 – 672.
- 36 S. Channiwala and P. Parikh, *Fuel*, 2002, **81**, 1051 – 1063.
- 37 L. Waldheim and T. Nilsson, *Heating value of gases from biomass gasification*, Iea bioenergy technical report, 2001.
- 38 S. Ghysels, A. E. E. Léon, M. Pala, K. A. Schoder, J. V. Acker and F. Ronsse, *Chem. Eng. J.*, 2019, **373**, 446 – 457.
- 39 C. Mohabeer, L. Abdelouahed, S. Marcotte and B. Taouk, *J. Anal. Appl. Pyrol.*, 2017, **127**, 269 – 277.
- 40 Y. Zheng, R. Grant, W. Hu and S. A. Scott, *Chem. Eng. J.*, 2019, **355**, 858 – 870.
- 41 D. Argüello, E. Chavez, F. Laurysen, R. Vanderschueren, E. Smolders and D. Montalvo, *Sci. Total Environ.*, 2019, **649**, 120 – 127.
- 42 A. Gramlich, S. Tandy, C. Gauggel, M. López, D. Perla, V. Gonzalez and R. Schulin, *Sci. Total Environ.*, 2018, **612**, 370 – 378.
- 43 C. Telmo, J. Lousada and N. Moreira, *Bioresource Technol.*, 2010, **101**, 3808 – 3815.
- 44 P. D. Muley, C. Henkel, K. K. Abdollahi, C. Marculescu and D. Boldor, *Energ. Convers. Manage.*, 2016, **117**, 273 – 280.
- 45 A. Ozyuguran, A. Akturk and S. Yaman, *Fuel*, 2018, **214**, 640 – 646.
- 46 A. M. Buswell and H. F. Mueller, *Ind. Eng. Chem.*, 1952, **44**, 550–552.
- 47 N. Acosta, *PhD thesis*, Ghent University, 2019.
- 48 K. Wang, C. He, S. You, W. Liu, W. Wang, R. Zhang, H. Qi and N. Ren, *J. Hazard. Mater.*, 2015, **300**, 745 – 753.
- 49 M. T. Reza, S. R. Poulson, S. Román and C. J. Coronella, *J. Anal. Appl. Pyrol.*, 2018, **131**, 85 – 92.
- 50 R. V. Poucke, S. Allaert, Y. Ok, M. Pala, F. Ronsse, F. Tack and E. Meers, *J. Environ. Manage.*, 2019, **246**, 496 – 504.
- 51 H. Yang, R. Yan, H. Chen, D. H. Lee and C. Zheng, *Fuel*, 2007, **86**, 1781 – 1788.
- 52 K. Weber and P. Quicker, *Fuel*, 2018, **217**, 240 – 261.
- 53 R. Venderbosch and W. Prins, *Biofuel. Bioprod. Bior.*, 2010, **4**, 178–208.
- 54 O. D. Mante, S. J. Thompson, S. Mustapha and D. C. Dayton, *Green Chem.*, 2019, **21**, 2257–2265.
- 55 Q. Yan, X. Liu, Y. Wang, H. Li, Z. Li, L. Zhou, Y. Qu, Z. Li and X. Bao, *AMB Express*, 2018, **8**, year.
- 56 W. Liu, H. Jiang and H. Yu, *Chem. Rev.*, 2015, **115**, 12251–12285.
- 57 L. Zhu, Y. Zhang, H. Lei, X. Zhang, L. Wang, Q. Bu and Y. Wei, *Sustainable Energy Fuels*, 2018, **2**, 1781–1790.
- 58 H. Lu and X. S. Zhao, *Sustainable Energy Fuels*, 2017, **1**, 1265–1281.
- 59 K. Crombie and O. Mašek, *Bioresource Technol.*, 2014, **162**, 148 – 156.
- 60 J. González-Arias, C. Fernández, J. Rosas, M. Bernal, R. Clemente, M. Sánchez and X. Gómez, *Waste Biomass Valori.*, 2019.
- 61 A. Del Giudice, A. Acampora, E. Santangelo, L. Pari, S. Bergonzoli, E. Guerriero, F. Petracchini, M. Torre, V. Paolini and F. Gallucci, *Energies*, 2019, **12**, year.
- 62 C. Amen-Chen, H. Pakdel and C. Roy, *Biomass Bioenerg.*, 1997, **13**, 25 – 37.
- 63 M. Gallucci, M. Carezzano, M. Oliva, M. Demo, R. Pizzolitto, M. Zunino, J. Zygodlo and J. Dambolena, *J. Appl. Microbiol.*, 2014, **116**, 795–804.
- 64 K. H. Nicastro, C. J. Kloxin and T. H. Epps, *ACS Sustain. Chem. Eng.*, 2018, **6**, 14812–14819.
- 65 N. Mahmood, Z. Yuan, J. Schmidt and C. C. Xu, *Renew. Sust. Energ. Rev.*, 2016, **60**, 317 – 329.
- 66 S. Hosseinneshad, E. H. Fini, B. K. Sharma, M. Basti and B. Kunwar, *RSC Adv.*, 2015, **5**, 75519–75527.
- 67 Y. Huang, Y. Duan, S. Qiu, M. Wang, C. Ju, H. Cao, Y. Fang and T. Tan, *Sustain. Energ. Fuels*, 2018, **2**, 637–647.
- 68 I. Borghol, C. Queffélec, P. Bolle, J. Descamps, C. Lombard, O. Lépine, D. Kucma, C. Lorentz, D. Laurenti, V. Montouillout, E. Chailleux and B. Bujoli, *Green Chem.*, 2018, **20**, 2337–2344.